

# Bolometric arrays and infrared sensitivity of VO<sub>2</sub> films with varying stoichiometry

Y. Hu,<sup>1</sup> C. H. Lin,<sup>1</sup> S. Min,<sup>1,2</sup> R. L. Smith<sup>2</sup> and S. Roberts<sup>2</sup>

<sup>1</sup>Wuhan Polytechnic University, Wuhan, China, <sup>2</sup>Rio Salado College, Tempe, AZ, USA

Journal of Optoelectronics and Materials Engineering 8, 345 (2017)

## Abstract

Here we propose a linear microbolometric array based on VO<sub>x</sub> thin films. The linear microbolometric array is fabricated by using micromachining technology, and its thermo-sensitive VO<sub>x</sub> thin film has excellent infrared response spectrum and TCR characteristics. Nano-scale VO<sub>x</sub> thin films deposited on SiO<sub>2</sub>/Si substrates were obtained by e-beam vapor deposition. The VO<sub>x</sub> films were then annealed at temperatures between 300 to 500 °C with various deposition duration time. The crystal structures and microstructures were examined by XRD, SEM and ESCA. These films showed a predominant phase of rhombohedral VO<sub>2</sub> and the crystallinity of the VO<sub>2</sub> increased as the annealing temperature increased. Integrated with CMOS circuit, an experimentally prototypical monolithic linear microbolometric array is designed and fabricated. The testing results of the experimental linear array show that the responsivity of linear array can approach 18KV/W and is potential for infrared image systems.

## 1. Introduction

In recent years, resistive random access memory (RRAM) devices have more and more attentions because of its advantages, such as low power requirement, fast switching speed, and small size [1-30]. RRAM was made of sandwiched, metal-insulator-metal (MIM), structure. The resistive switching behavior in most of the transition metal oxide (TMO) –based RRAMs was explained by filamentary model [4], where the change of resistance from high resistive state (off-state) to low resistive state (on- state) is called the set process, and the anti-process is called reset process. According to I-V curve of the RRAM device, when set and reset process appear at the same quadrant, the resistive switching behavior was classified as unipolar resistive switch (URS), if not, the resistive switching behavior was classified as bipolar resistive switch (BRS) [31-70]. VO<sub>2</sub> has been studied several years, since F. J. Morin found its semiconductor-to-metal transition temperature  $T_t = 340$  K in 1959. This transition property makes VO<sub>2</sub> good applications for encompassing thermochromic coatings, optical and holographic storage systems, fiber optical switching devices, and laser scanners, but not for RRAMs. [71-140]

Microbolometric arrays have more advantages such as higher stability, reduced power dissipation, smaller size and lighter weight than conventional cooled infrared detector arrays. Development work on

microbolometric arrays has focused on improving their sensitivity. One of key methods for improving microbolometric sensitivity is through mending the process of fabricating microbolometers to increase their temperature coefficient of resistance (TCR) values. Since the phase-transition phenomenon of vanadium dioxides (VO<sub>2</sub>) materials was first observed in the late 1950s, many researchers have been interested in VO<sub>2</sub> thin films. Early tests of TCR indicated that the films of VO<sub>2</sub> would perform better than a metal TCR resistor, furthermore the TCR values of VO<sub>2</sub> thin films can be controlled by adjusting their ingredients. In addition, thin films of VO<sub>2</sub> are selected for microbolometric arrays because the fabricating technology of VO<sub>2</sub> thin films is compatible with integrated circuit (IC) process, which is favorable to designing and fabricating monolithic microbolometric arrays.

Table 1: The process flow details

Target	V <sub>2</sub> O <sub>5</sub> powder
Pre-evaporating Time	3 min
Evaporating Time	20 sec
Emission	53 %
Pressure	5x10 <sup>-5</sup> Torr
Substrate Temperature	32 °C

The performance of VO<sub>2</sub>-based microbolometric arrays depends on not only the TCR of VO<sub>2</sub> thin films but also the structure of microbolometers and the performance of the readout integrated circuit. For linear microbolometric array, the simple structure of conventional micro-bridge is unfavorable to microbolometric sensitivity. The conventional micro-bridge structure for linear microbolometric arrays is shown in Fig. 1, in which the thermal conductance of the supporting legs is fairly large and can lower the microbolometric sensitivity. Besides, it is also a challenge to achieve good performance of the readout integrated circuit. In this paper, a new linear microbolometric array based on vanadium oxides (VO<sub>x</sub>) thin film is designed and fabricated. Integrated with complementary metal oxide semiconductor (CMOS) readout integrated circuit, the VO<sub>x</sub> microbolometers in linear array has more perfect structure compared with conventional micro-bridge structure for linear array and excellent TCR characteristics. The experimental monolithic linear arrays based on VO<sub>x</sub> thin film reveal good performance and can be applied to practical infrared image systems.

## 2. Experimental details and Fabrication

We used Si (100) wafer which was oxidized in a furnace to grow a SiO<sub>2</sub> insulator layer as the substrate. Bottom electrodes of Pt were patterned with a shadow mask by sputter. The evaporating target was made of V<sub>2</sub>O<sub>5</sub> powder, and then we deposited VO<sub>x</sub> thin films on Pt/SiO<sub>2</sub>/Si substrate under 5×10<sup>-5</sup> torr for 20 second by evaporator. The coating conditions were shown in Table 1. After evaporating VO<sub>x</sub> thin films, we used Rapid Thermal Annealing (RTA) to anneal VO<sub>x</sub> thin films under 10 mtorr at different temperatures (300/400/450/500 °C) for 1 minute. The top Pt electrodes were deposited on VO<sub>x</sub> thin films at the end. The crystalline structure of VO<sub>x</sub> thin films were determined by X-ray diffraction (XRD). The binding energy of V<sub>2</sub>O<sub>3</sub> thin films were measured by Electron Spectroscopy for Chemical Analysis (ESCA). The cross-sectional morphology of the V<sub>2</sub>O<sub>3</sub>/SiO<sub>2</sub>/Si structure was obtained using a Field Emission Scanning Electron Microscopy (FESEM). The resistive switching behaviors of metal-insulator-metal (MIM) devices were measured by Keithley-4200.

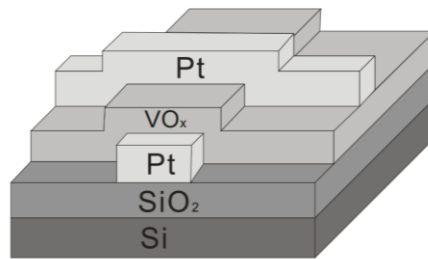


Fig. 1: Schematic of the device structure described in the text.

In order to improve the sensitivity of microbolometer, a standard micro-bridge structure which is widely utilized in microbolometric focal plane arrays is used for microbolometer pixel [6, 7]. The micro-bridge structure of VO<sub>x</sub> bolometer is illustrated in Fig. 2. The microbolometer consists of a 0.5 μm thick micro-bridge of Si<sub>3</sub>N<sub>4</sub> suspended above the underlying silicon substrate, two narrow legs of Si<sub>3</sub>N<sub>4</sub> which are 2.0 μm high and supporting the bridge, and a 100×100 μm thin film (0.5 μm thick) of VO<sub>x</sub> which is encapsulated in the center of the micro-bridge. The basic operational principal of the microbolometer is as follows. When the VO<sub>x</sub> thin film is irradiated by infrared (IR) radiation and heated, its resistance value is changed. This change in the resistance value of the VO<sub>x</sub> thin film can be converted to voltage signal to be output through the CMOS readout integrated circuit in silicon substrate, which is connecting to the narrow legs via the X or Y metal on the surface of silicon substrate. From Fig. 2, it can be found that the two supporting legs are narrow and clival.

This kind of supporting legs is in favor of the microbolometer heat isolation from silicon substrate, so the IR heating efficiency on the VO<sub>x</sub> thin film is high, which can greatly improve microbolometric sensitivity.

The micro-bridge structure microbolometer is produced in a way using a surface micromachining technique. Figure 3 illustrates the six fabrication steps of a micro-bridge structure microbolometer. Fabrication begins with implantation of the required CMOS readout electronics and conducting metallizations in the silicon wafer. The wafer is then planarized with the spun-on polyimide, which is photolithographically patterned to form sacrificial mesa. Over the sacrificial mesa the silicon nitride layer is sputtered together with subsequent  $\text{VO}_x$  thin film. Subsequently, together with connecting metallizations the silicon nitride protecting layer is sputtered. And as a final step, the sacrificial mesa is removed by oxygen plasma etching to leave a self-supporting micro-bridge structure.

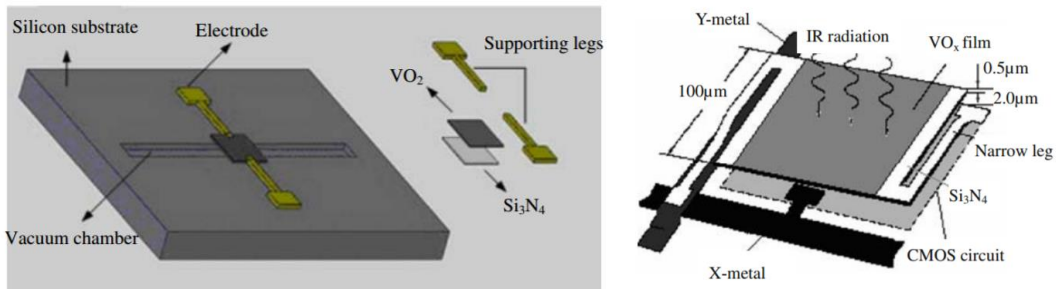


Fig. 2: (left) Schematic of the device fabrication process and (right) magnified view of the crab-leg structure.

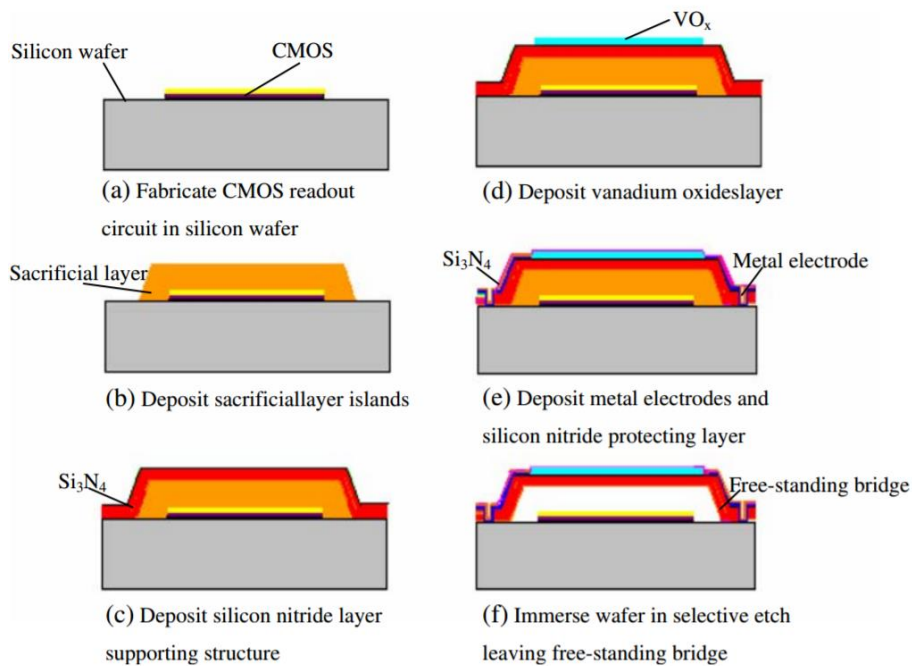


Fig. 3: Illustration of the process flow.

### 3. Results and discussions

The micro-bridge structure design allows great fill factor for the CMOS readout integrated circuit is placed in the silicon underneath the micro-bridge and great IR absorption for the underlying cavity produces a resonant optical cavity. So this type of micro-bridge structure design can improve the whole performance of linear array including increasing microbolometric sensitivity and decreasing noise equivalent temperature difference, that is to say that little IR radiation power from target can produce great resistance change of the VOx thin film. Among the components of micro-bridge structure microbolometer, the photoelectric properties of VOx thin film are vital, and the VOx thin film fabricated in our laboratory has excellent optical and electrical properties. On the fourth step in the fabricating processes of microbolometer, a thin film of vanadium produced at first undergoes a chemical reaction by being annealed, which leads to form the VOx thin film. In fact, the annealing is in Ar and O<sub>2</sub>, so the formed thin film consists of VOx consequentially. Because the relationship curve of temperature-resistance of the thin film is different from the relationship curve of VO<sub>2</sub> material [3], the thin film does not consist of VO<sub>2</sub> material only. X-ray diffraction (XRD) measurement makes it clear that the thin films contain V<sub>2</sub>O<sub>3</sub> except for VO<sub>2</sub> rather than VO<sub>2</sub> only. This is showed in Fig. 4, from which it is found that the VOx thin film is the mixture of VO<sub>2</sub> and V<sub>2</sub>O<sub>3</sub>. Experiments demonstrate that the different annealing temperature and time can result in the different amount of V<sub>2</sub>O<sub>3</sub> material contained in the VO<sub>2</sub> thin film, so the fabricating process of VOx is essentially a process which is adjusting the ingredients of the thin film. The long wave infrared spectrum absorptivity of the VOx thin film, in the 8.0–15.0 μm wavelength range, is shown in Fig. 5.

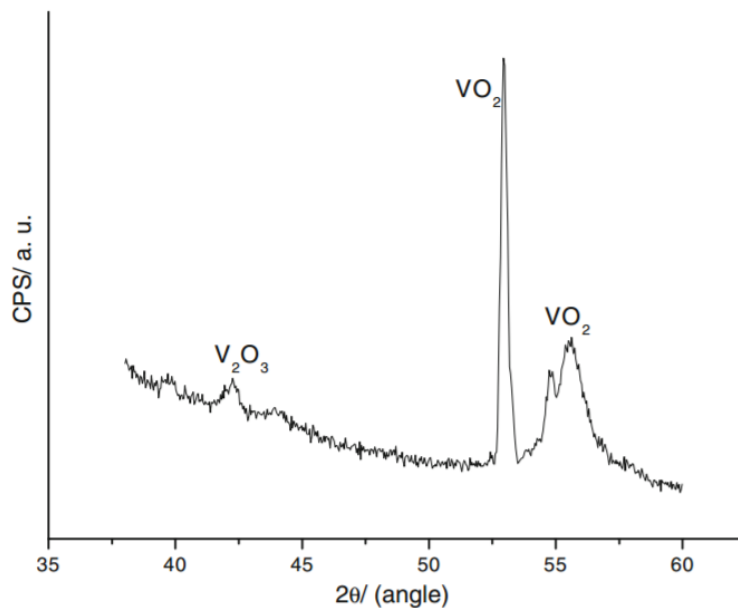


Fig. 4: XRD spectrum of the VO<sub>2</sub> film.

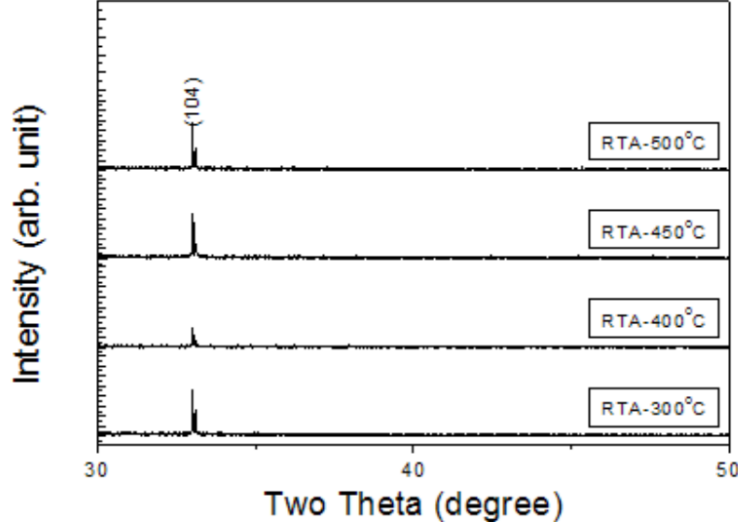


Fig. 5: XRD of the VO<sub>2</sub> films at different RTA temperatures used.

It can be found that the VO<sub>x</sub> thin film has very high infrared absorptivity in long wave infrared spectrum. At the same time, measurement shows that the VO<sub>x</sub> thin film has excellent temperature-resistance characteristic. Figure 6 shows the curve of sheet resistance versus temperature for the VO<sub>x</sub> thin film, from which it can be found that the TCR of the VO<sub>x</sub> thin film reaches to  $-2.7\%$  at room temperature and is higher than that of traditional VO<sub>2</sub> thin film (about  $-2.0\%$ ) [2]. In addition, the CMOS readout integrated circuit of the linear array adopts a combined readout structure of bolometer current direct injection (BCDI) and capacitor feedback transimpedance amplifier (CTIA). The CMOS readout integrated circuit is shown in Fig. 7. The BCDI input circuit is formed by the bolometer  $R_d$  (when exposed to infrared light, its resistance can be changed), the blind bolometer  $R_b$  (not exposed to infrared light), the PMOS device P1 and the NMOS devices N1. The CTIA integrated circuit contains the reset switch N2, the integration capacitor  $C_{int}$ , and the amplifier A. The blind bolometer  $R_b$  can cancel the bias current contained in the bolometer  $R_d$  and depress the affection of substrate temperature fluctuation, the MOS devices N1 and P1 are a pair of complementary integration controlling switches, which are utilized to control the integration time of the photon-generated current  $I_{int}$ , and the CTIA provides a highly stable bias to the detector and has high-performances such as high-gain, high photon current injection efficiency and low noise. The circuit operation is explained as follows. When the pair of integration controlling switches N1 and P1 are ON and the reset switch N2 is OFF, the photon-generated current  $I_{int}$  is integrated into the integration capacitor  $C_{int}$ . After an integrating interval, the pair of integration controlling switches N1 and P1 turn off and the readout voltage signal  $V_{out}$  is output.

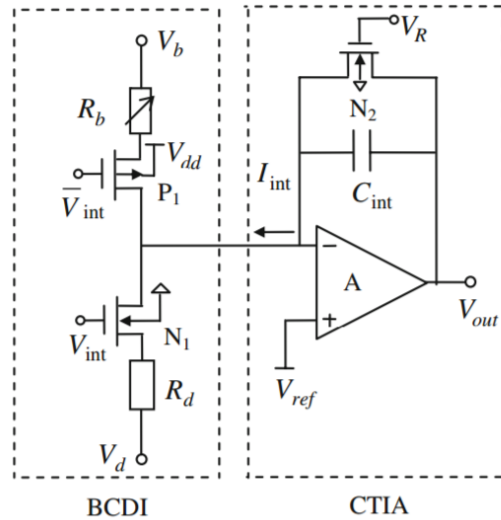


Fig. 6: Circuit schematic of the bolometer.

An experimental monolithic chip for  $100 \times 100 \mu\text{m}$ -pitch 128 element linear microbolometric array has been designed and fabricated to verify the designed linear array based on VOx thin film. The micrograph of two typical microbolometers in the linear array is shown in Fig. 8. This linear array is designed to work under 5 V power supplies, packaged in vacuum and tested under a 298 K environment. The voltage responsivity of the linear array is defined in Equation 1 where  $d$  is the number of bad and dead detectors, and  $R_v(I)$  is the voltage responsivity of the microbolometer No.  $I$  and expressed as  $R_v \propto I^{1/4} V_{out} \propto I^{1/4} P$  in which  $V_{out}(I)$  is the output voltage of the microbolometer No.  $I$  heated by infrared irradiation power  $P$ . Measurements show that the zero-frequency voltage responsivity of the linear array is the function of bias current in microbolometer which is illustrated in Fig. 9. When the bias current increases above  $20 \mu\text{A}$ , the zero-frequency voltage responsivity is almost constant (approximately about  $18 \text{KV/W}$ ), but being accompanied with gradually increasing noise. By maintaining  $20 \mu\text{A}$  bias current, the voltage responsivity at different frequencies is obtained. The relationship between voltage responsivity and frequency is shown Fig. 10, from which it can be found that the voltage responsivity declines with the increase of signal frequency. The Nyquist frequency of the voltage responsivity is about 10 Hz, which is consistent with designed response time characteristic.

Fig. 1 shows a part of metal- insulator-metal (MIM) structure. Fig. 2 shows that the XRD patterns of the VOx thin films that they were deposited on Pt/SiO<sub>2</sub>/Si substrate annealed at different temperature (300/400/450/500 °C) by RTA. All of thin films showed the same orientation peak at  $2\theta=33.0^\circ$  which were matched with JCPDS card No. 85-1411. Basing on the result that all of thin films were V<sub>2</sub>O<sub>3</sub> with rhombohedral structure. Fig. 3 is the ESCA patterns of the VOx thin films which were annealed at 300/400/450/500 °C by RTA.

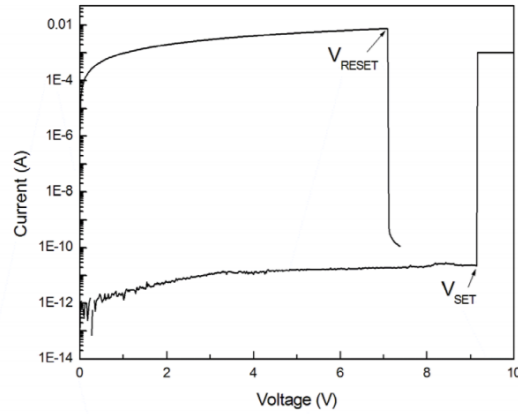


Fig. 7: Current-voltage curves showing the set and reset process

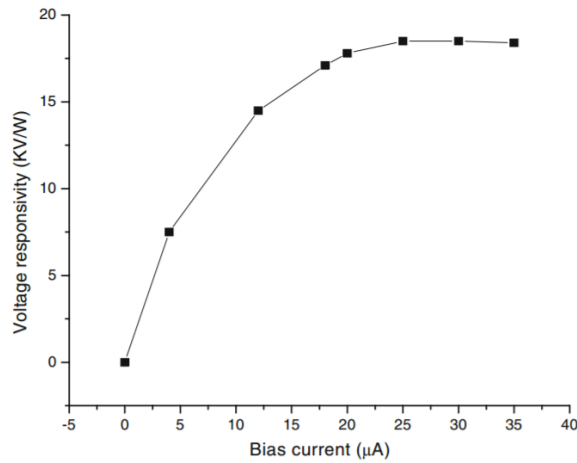


Fig. 8: Voltage responsivity against bias current.

The peaks at 516.3 eV are the binding energy of V2O3 where the valence state of V is V+1.5. The SEM of the V2O3 surface morphology annealed at 400 °C was shown in Fig. 4. The surface of V2O3 thin film was smooth, and there do not appear obviously crystal particles. Fig. 5 shows the cross section of V2O3 films annealed at (a) 300 (b) 400 (c) 450 (d) 500 °C by RTA. The thickness of V2O3 thin films were about 150~200 nm, and there had fine V2O3/SiO2 interface. Fig. 6 shows the resistive switching characteristics of Pt/ V2O3/Pt/SiO2/Si device where V2O3 thin films were annealed at 400 °C for 1 minute by RTA. It shows that the  $I_{max}$  ( $V_{reset}$ ) is  $7.93 \times 10^{-3}$  A, and  $I_{set}$  ( $V_{set}$ ) is  $2.26 \times 10^{-11}$  A, the current range between  $V_{reset}$  to  $V_{set}$  is about 7 orders. Summary We observed the thin film with rhombohedral structure after annealing at different temperatures by RTA. The thickness of the thin films is about 150~200 nm depended on the deposition duration times. In this work, we found the device with Pt/V2O3/Pt structures annealed at 400 °C exhibit the largest memory window. The range of the memory window (ION to IOFF) achieved nine



orders. The mechanism of the resistive switching behavior of the V2O3 thin film was explained by the filamentary model.

#### 4. Conclusions

A linear microbolometric array based on VOx thin film has been fabricated by using a new micromachining process, which consists of six steps. The benefit of the new micromachining process is to improve the microbolometric sensitivity and this leads to high voltage responsivity of the linear microbolometric array. We expect the linear micro-bolometric array based on VOx thin film will play an important role in developing potential civil and military applications. Further investigations on improving the performance characteristics such as noise equivalent temperature difference and nonuniformity are in progress.

#### References

- [1] Amelinckx, S., A. A. Lucas, and Ph. Lambin, 1999a, in *The Science and Technology of Carbon Nanotubes*, edited by K. Tanaka, T. Yamabe, and K. Fukui (Elsevier Science, Amsterdam), p. 14.
- [2] Amelinckx, S., A. A. Lucas, and Ph. Lambin, 1999b, "Electron diffraction and microscopy of nanotubes," *Rep. Prog. Phys.* **62**, 1.
- [3] Bernaerts, D., X. B. Zhang, X. F. Zhang, S. Amelinckx, G. Van Tendeloo, J. Van Landuyt, V. Yvanov, and J. B'Nagy, 1995, "Electron microscopy study of coiled carbon nanotubes," *Philos. Mag. A* **71**, 605.
- [4] Kumar, S., 2012, "Fundamental limits to Moore's law," Stanford University, <http://large.stanford.edu/courses/2012/ph250/kumar1/>
- [5] Bragg, W. L., 1939, "A new kind of "x-ray microscope," " *Nature (London)* **143**, 678.
- [6] Bragg, W. L., 1944, "Lightning calculations with light," *Nature (London)* **154**, 69.
- [7] Curl, R. F., and R. E. Smalley, 1991, "Fullerenes: The third form of pure carbon," *Sci. Am.* **264**, 54.
- [8] Dekker, C., 1999, "Carbon nanotubes as molecular quantum wires," *Phys. Today* **52** (5), 22.
- [9] Ebbesen, T. W., 1994, "Carbon nanotubes," *Annu. Rev. Mater. Sci.* **24**, 235.
- [10] Ebbesen, T. W., 1996, "Carbon nanotubes," *Phys. Today* **49** (6), 26.
- [11] Ebbesen, T. W., and P. M. Ajayan, 1992, "Large-scale synthesis of carbon nanotubes," *Nature (London)* **358**, 220.
- [12] Henrard, L., E. Hernández, P. Bernier, and A. Rubio, 1999, "van der Waals interaction in nanotube bundles: Consequences on vibrational modes," *Phys. Rev. B* **60**, R8521.
- [13] Huffman, D. R., 1991, "Solid C60," *Phys. Today* **44**, 22.
- [14] Iijima, S., 1991, "Helical microtubules of graphitic carbon," *Nature (London)* **354**, 56.
- [15] Iijima, S., 1994, "Carbon nanotubes," *MRS Bull.* **19**, 43.
- [16] Krätschmer, W., L. D. Lamb, K. Fostiropoulos, and D. R. Huffman, 1990, "Solid C60: A new form of carbon," *Nature (London)* **347**, 354.
- [17] Kumar, S., 2011, "Superconductors for electrical power," Stanford University, <http://large.stanford.edu/courses/2011/ph240/kumar1/>
- [18] Kroto, H. W., J. R. Heath, S. C. O'Brien, R. F. Curl, and R. E. Smalley, 1985, "C60: Buckminsterfullerene," *Nature (London)* **318**, 162.
- [19] Lambin, Ph., and A. A. Lucas, 1997, "Quantitative theory of diffraction by carbon nanotubes," *Phys. Rev. B* **56**, 3571.
- [20] Léonard, F., and J. Tersoff, 2000, "Negative differential resistance in nanotube devices," *Phys. Rev. Lett.* **85**, 4767.
- [21] Lisensky, G. C., T. F. Kelly, D. R. Neu, and A. B. Ellis, 1991, "The optical transform. Simulating diffraction experiments in introductory courses," *J. Chem. Educ.* **68**, 91.
- [22] Loiseau, A., F. Willaime, N. Demoncey, G. Hug, and H. Pascard, 1996, "Boron nitride nanotubes with reduced numbers of layers synthesized by arc discharge," *Phys. Rev. Lett.* **76**, 4737.
- [23] Lucas, A. A., Ph. Lambin, R. Mairesse, and M. Mathot, 1999, "Revealing the backbone structure of B-DNA from laser optical simulations of its x-ray diffraction diagram," *J. Chem. Educ.* **76**, 378.
- [24] Meunier, V., L. Henrard, and Ph. Lambin, 1998, "Energetics of bent carbon nanotubes," *Phys. Rev. B* **57**, 2586.
- [25] Moreau, F., Ph. Lambin, A. A. Lucas, J. C. Dore, *et al.*, 2001, "Neutron diffraction analysis of a nanotube powder produced by arc discharge," *Phys. Rev. B* (in press).
- [26] Qin, L. C., 1994, "Electron diffraction from cylindrical nanotubes," *J. Mater. Res.* **9**, 2450.
- [27] Qin, L. C., T. Ichihashi, and S. Iijima, 1997, "On the measurement of helicity of carbon nanotubes," *Ultramicroscopy* **67**, 181.

- [28] Kumar, S., Esfandyarpour, R., Davis, R., Nishi, Y., 2014, "Surface charge sensing by altering the phase transition in VO<sub>2</sub>," *Journal of Applied Physics* 116, 074511. <http://scitation.aip.org/content/aip/journal/jap/116/7/10.1063/1.4893577>
- [29] Kumar, S., Esfandyarpour, R., Davis, R., Nishi, Y., 2014, "Charge sensing by altering the phase transition in VO<sub>2</sub>," *APS March Meeting Abstracts* 1, 1135.
- [30] Tanaka, K., T. Yamabe, and K. Fukui, editors, 1999, in *The Science and Technology of Carbon Nanotubes* (Elsevier Science, Amsterdam).
- [31] Tenne, R., L. Margulis, M. Genut, and G. Hodes, 1992, "Polyhedral and cylindrical structures of tungsten disulfide," *Nature (London)* **360**, 444.
- [32] Zhen, Y., H. Ch. Postma, L. Balents, and C. Dekker, 1999, "Carbon nanotube intramolecular junctions," *Nature (London)* **402**, 273.
- [33] Cappelluti, E., L. Benfatto, and A. B. Kuzmenko, 2010, "Phonon switching and combined Fano-Rice effect in optical spectra of bilayer graphene," *Phys. Rev. B* **82**, 041402(R).
- [34] Carbotte, J. P., J. P. F. LeBlanc, and E. J. Nicol, 2012, "Emergence of Plasmaronic Structure in the Near Field Optical Response of Graphene," *Phys. Rev. B* **85**, 201411(R).
- [35] Casiraghi, C., A. Hartschuh, H. Qian, S. Piscanec, C. Georgi, A. Fasoli, K. S. Novoselov, D. M. Basko, and A. C. Ferrari, 2009, "Raman Spectroscopy of Graphene Edges," *Nano Lett.* **9**, 1433.
- [36] Castro, Eduardo V., K. S. Novoselov, S. V. Morozov, N. M. R. Peres, J. M. B. Lopes dos Santos, Johan Nilsson, F. Guinea, A. K. Geim, and A. H. Castro Neto, 2007, "Biased Bilayer Graphene: Semiconductor with a Gap Tunable by the Electric Field Effect," *Phys. Rev. Lett.* **99**, 216802.
- [37] Castro Neto, A. H., and F. Guinea, 2009, "Impurity-Induced Spin-Orbit Coupling in Graphene," *Phys. Rev. Lett.* **103**, 026804.
- [38] Castro Neto, A. H., F. Guinea, N. M. R. Peres, K. S. Novoselov, and A. K. Geim, 2009, "The electronic properties of graphene," *Rev. Mod. Phys.* **81**, 109.
- [39] Chae, Dong-Hun, Tobias Utikal, Siegfried Weisenburger, Harald Giessen, Klaus v. Klitzing, Markus Lippitz, and Jurgen Smet, 2011, "Excitonic Fano Resonance in Free-Standing Graphene," *Nano Lett.* **11**, 1379.
- [40] Chae, Jungseok, *et al.*, 2012, "Renormalization of the Graphene Dispersion Velocity Determined from Scanning Tunneling Spectroscopy," *Phys. Rev. Lett.* **109**, 116802.
- [41] Charrier, A., A. Coati, T. Argunova, F. Thibaudau, Y. Garreau, R. Pinchaux, I. Forbeaux, J.-M. Debever, M. Sauvage-Simkin, and J.-M. Themlin, 2002, "Solid-state decomposition of silicon carbide for growing ultra-thin heteroepitaxial graphite films," *J. Appl. Phys.* **92**, 2479.
- [42] Chatzakis, Ioannis, Hugen Yan, Daohua Song, Stéphane Berciaud, and Tony F. Heinz, 2011, "Temperature dependence of the anharmonic decay of optical phonons in carbon nanotubes and graphite," *Phys. Rev. B* **83**, 205411.
- [43] Cheianov, V. V., V. I. Fal'ko, B. L. Altshuler, and I. L. Aleiner, 2007, "Random Resistor Network Model of Minimal Conductivity in Graphene," *Phys. Rev. Lett.* **99**, 176801.
- [44] Cheianov, Vadim V., Vladimir Fal'ko, and B. L. Altshuler, 2007, "The Focusing of Electron Flow and a Veselago Lens in Graphene p-n Junctions," *Science* **315**, 1252.
- [45] Chen, Chi-Fan, *et al.*, 2011, "Controlling inelastic light scattering quantum pathways in graphene," *Nature (London)* **471**, 617.
- [46] Chen, J.-H., C. Jang, S. Adam, M. S. Fuhrer, E. D. Williams, and M. Ishigami, 2008, "Charged-impurity scattering in graphene," *Nat. Phys.* **4**, 377.
- [47] Chen, Jianing, *et al.*, 2012, "Optical nano-imaging of gate-tunable graphene plasmons," *Nature (London)* **487**, 77.
- [48] Chiu, K. W., and J. J. Quinn, 1974, "Plasma oscillations of a two-dimensional electron gas in a strong magnetic field," *Phys. Rev. B* **9**, 4724.
- [49] Kumar, S., 2011, "Energy from radioactivity," Stanford University, <http://large.stanford.edu/courses/2011/ph240/kumar2/>
- [50] Kumar, S., 2015, "Atomic Batteries: Energy from radioactivity," arXiv:1511.07427, <http://arxiv.org/abs/1511.07427>
- [51] Choi, H., F. Borondics, D. A. Siegel, S. Y. Zhou, M. C. Martin, A. Lanzara, and R. A. Kaindl, 2009, "Broadband electromagnetic response and ultrafast dynamics of few-layer epitaxial graphene," *Appl. Phys. Lett.* **94**, 172102.
- [52] Coletti, C., C. Riedl, D. S. Lee, B. Krauss, L. Patthey, K. von Klitzing, J. H. Smet, and U. Starke, 2010, "Charge neutrality and band-gap tuning of epitaxial graphene on SiC by molecular doping," *Phys. Rev. B* **81**, 235401.
- [53] Connolly, M. R., K. L. Chiou, C. G. Smith, D. Anderson, G. A. C. Jones, A. Lombardo, A. Fasoli, and A. C. Ferrari, 2010, "Scanning gate microscopy of current-annealed single layer graphene," *Appl. Phys. Lett.* **96**, 113501.
- [54] Connolly, M. R., and C. G. Smith, 2010, "Nanoanalysis of graphene layers using scanning probe techniques," *Phil. Trans. R. Soc. A* **368**, 5379.
- [55] Crassee, I., J. Levallois, D. van der Marel, A. L. Walter, Th. Seyller, and A. B. Kuzmenko, 2011, "Multicomponent magneto-optical conductivity of multilayer graphene on SiC," *Phys. Rev. B* **84**, 035103.
- [56] Crassee, I., M. Orlita, M. Potemski, A. L. Walter, M. Ostler, Th. Seyller, I. Gaponenko, J. Chen, and A. B. Kuzmenko, 2012, "Intrinsic Terahertz Plasmons and Magnetoplasmons in Large Scale Monolayer Graphene," *Nano Lett.* **12**, 2470.
- [57] Kumar, S., 2014, "Mechanisms of Resistance Switching in Various Transition Metal Oxides," Stanford University.
- [58] Crassee, Iris, Julien Levallois, Andrew L. Walter, Markus Ostler, Aaron Bostwick, Eli Rotenberg, Thomas Seyller, Dirk van der Marel, and Alexey B. Kuzmenko, 2011, "Giant Faraday rotation in single- and multilayer graphene," *Nat. Phys.* **7**, 48.

- [59] Daimon, H., S. Imada, H. Nishimoto, and S. Suga, 1995, "Structure factor in photoemission from valence band," *J. Electron Spectrosc. Relat. Phenom.* **76**, 487.
- [60] S. Kumar et. al., 2016, "Smart packaging of electronics and integrated MEMS devices using LTCC," arXiv:1605.01789
- [61] Dan, Yaping, Ye Lu, Nicholas J. Kybert, Zhengtang Luo, and A. T. Charlie Johnson, 2009, "Intrinsic Response of Graphene Vapor Sensors," *Nano Lett.* **9**, 1472.
- [62] Das, A., et al., 2008, "Monitoring dopants by Raman scattering in an electrochemically top-gated graphene transistor," *Nat. Nanotechnol.* **3**, 210.
- [63] Das Sarma, S., Shaffique Adam, E. H. Hwang, and Enrico Rossi, 2011, "Electronic transport in two-dimensional graphene," *Rev. Mod. Phys.* **83**, 407.
- [64] S. Kumar, et. al., 2016, "The phase transition in VO<sub>2</sub> probed using x-ray, visible and infrared radiations," *Applied Physics Letters*, 108, 073102
- [65] Das Sarma, S., and E. H. Hwang, 2013, "Velocity renormalization and anomalous quasiparticle dispersion in extrinsic graphene," *Phys. Rev. B* **87**, 045425.
- [66] Das Sarma, S., E. H. Hwang, and Wang-Kong Tse, 2007, "Many-body interaction effects in doped and undoped graphene: Fermi liquid versus non-Fermi liquid," *Phys. Rev. B* **75**, 121406(R).
- [67] Jayamurugan, G, Vasu, K. S., Rajesh, Y. B. R. D., Kumar, S., Vasumathi, V., Maiti, P. K., Sood, A. K., Jayaraman, N., 2011, "Interaction of single-walled carbon nanotubes with poly (propyl ether imine) dendrimers," *J. Chem. Phys.* **134**, 104507.
- [68] Dawlaty, Jahan M., Shriram Shivaraman, Mvs Chandrashekar, Farhan Rana, and Michael G. Spencer, 2008, "Measurement of ultrafast carrier dynamics in epitaxial graphene," *Appl. Phys. Lett.* **92**, 042116.
- [69] Dean, C. R., et al., 2013, "Hofstadter's butterfly and the fractal quantum Hall effect in moiré superlattices," *Nature (London)* **497**, 598.
- [70] Dean, C. R., et al., 2010, "Boron nitride substrates for high-quality graphene electronics," *Nat. Nanotechnol.* **5**, 722.
- [71] Decker, Régis, Yang Wang, Victor W. Brar, William Regan, Hsin-Zon Tsai, Qiong Wu, William Gannett, Alex Zettl, and Michael F. Crommie, 2011a, "Local Electronic Properties of Graphene on a BN Substrate via Scanning Tunneling Microscopy," *Nano Lett.* **11**, 2291.
- [72] S. Kumar, "Mechanisms of resistance switching in various transition metal oxides," Thesis, Stanford University (2014)
- [73] Decker, Régis, Yang Wang, Victor W. Brar, William Regan, Hsin-Zon Tsai, Qiong Wu, William Gannett, Alex Zettl, and Michael F. Crommie, 2011b, "Local Electronic Properties of Graphene on a BN Substrate via Scanning Tunneling Microscopy," *Nano Lett.* **11**, 2291.
- [74] Dedkov, Yu. S., M. Fonin, U. Rüdiger, and C. Laubschat, 2008, "Rashba Effect in the Graphene/Ni(111) System," *Phys. Rev. Lett.* **100**, 107602.
- [75] de Heer, Walt A., Claire Berger, Ming Ruan, Mike Sprinkle, Xuebin Li, Yike Hu, Baiqian Zhang, John Hankinson, and Edward Conrad, 2011, "Large area and structured epitaxial graphene produced by confinement controlled sublimation of silicon carbide," *Proc. Natl. Acad. Sci. U.S.A.* **108**, 16 900.
- [76] de Heer, Walt A., et al., 2007, "Epitaxial graphene," *Solid State Commun.* **143**, 92.
- [77] Demel, T., D. Heitmann, P. Grambow, and K. Ploog, 1990, "Nonlocal dynamic response and level crossings in quantum-dot structures," *Phys. Rev. Lett.* **64**, 788.
- [78] Demel, T., D. Heitmann, P. Grambow, and K. Ploog, 1991, "One-dimensional plasmons in AlGaAs/GaAs quantum wires," *Phys. Rev. Lett.* **66**, 2657.
- [79] Deshpande, A., W. Bao, F. Miao, C. N. Lau, and B. J. LeRoy, 2009, "Spatially resolved spectroscopy of monolayer graphene on SiO<sub>2</sub>," *Phys. Rev. B* **79**, 205411.
- [80] Deshpande, A., W. Bao, Z. Zhao, C. N. Lau, and B. J. LeRoy, 2011, "Imaging charge density fluctuations in graphene using Coulomb blockade spectroscopy," *Phys. Rev. B* **83**, 155409.
- [81] S. Kumar, et. al., 2014, "Sequential electronic and structural transitions in VO<sub>2</sub> observed using x-ray absorption spectromicroscopy," *Advanced Materials*, **26**, 7505.
- [82] Dietl, Petra, Frédéric Piéchon, and Gilles Montambaux, 2008, "New Magnetic Field Dependence of Landau Levels in a Graphene-like Structure," *Phys. Rev. Lett.* **100**, 236405.
- [83] Dikin, Dmitriy A., Sasha Stankovich, Eric J. Zimney, Richard D. Piner, Geoffrey H. B. Dommett, Guennadi Evmenenko, SonBinh T. Nguyen, and Rodney S. Ruoff, 2007, "Preparation and characterization of graphene oxide paper," *Nature (London)* **448**, 457.
- [84] Dresselhaus, M. S., A. Jorio, L. G. Cançado, G. Dresselhaus, and R. Saito, 2012, "Raman Spectroscopy: Characterization of Edges, Defects, and the Fermi Energy of Graphene and sp<sup>2</sup> Carbons," in *Graphene Nanoelectronics: Metrology, Synthesis, Properties and Applications*, edited by Hasan Reza (Springer, Berlin), Chap. 2, p. 15.
- [85] Dresselhaus, Mildred S., Ado Jorio, Mario Hofmann, Gene Dresselhaus, and Riichiro Saito, 2010, "Perspectives on Carbon Nanotubes and Graphene Raman Spectroscopy," *Nano Lett.* **10**, 751.
- [86] Kumar, S., 2015, "Fundamental limits to Morre's law", arXiv:1511.05956, <http://arxiv.org/abs/1511.05956>
- [87] Drut, Joaquín E., and Timo A. Lähde, 2009, "Is Graphene in Vacuum an Insulator?" *Phys. Rev. Lett.* **102**, 026802.
- [88] Du, Xu, Ivan Skachko, Anthony Barker, and Eva Y. Andrei, 2008, "Approaching ballistic transport in suspended graphene," *Nat. Nanotechnol.* **3**, 491.
- [89] Eberlein, T., U. Bangert, R. R. Nair, R. Jones, M. Gass, A. L. Bleloch, K. S. Novoselov, A. Geim, and P. R. Briddon, 2008, "Plasmon spectroscopy of free-standing graphene films," *Phys. Rev. B* **77**, 233406.

- [90] Efetov, Dmitri K., and Philip Kim, 2010, "Controlling Electron-Phonon Interactions in Graphene at Ultrahigh Carrier Densities," *Phys. Rev. Lett.* **105**, 256805.
- [91] Efros, A. L., F. G. Pikus, and V. G. Burnett, 1993, "Density of states of a two-dimensional electron gas in a long-range random potential," *Phys. Rev. B* **47**, 2233.
- [92] Efros, A. L., and B. I. Shklovskii, 1984, *Electronic Properties of Doped Semiconductors* (Springer-Verlag, New York).
- [93] M. N. Suma, S. Kumar, 2009, "Performance Analysis and Process Parameters of Novel LTCC Filters," *International Journal of Recent Trends in Engineering*, 1, 346
- [94] Elias, D. C., *et al.*, 2011, "Dirac cones reshaped by interaction effects in suspended graphene," *Nat. Phys.* **7**, 701.
- [95] Eliasson, G., Ji-Wei Wu, P. Hawrylak, and J. J. Quinn, 1986, "Magnetoplasma modes of a spatially periodic two-dimensional electron gas," *Solid State Commun.* **60**, 41.
- [96] El-Kady, Maher F., Veronica Strong, Sergey Dubin, and Richard B. Kaner, 2012, "Laser Scribing of High-Performance and Flexible Graphene-Based Electrochemical Capacitors," *Science* **335**, 1326.
- [97] Kumar, S, 2012, "Learning from Solar Cells - Improving Nuclear Batteries," Stanford University, <http://large.stanford.edu/courses/2012/ph241/kumar2/>
- [98] Emtsev, Konstantin V., *et al.*, 2009, "Towards wafer-size graphene layers by atmospheric pressure graphitization of silicon carbide," *Nat. Mater.* **8**, 203.
- [99] Enderlein, C, Y. S Kim, A. Bostwick, E. Rotenberg, and K. Horn, 2010, "The formation of an energy gap in graphene on ruthenium by controlling the interface," *New J. Phys.* **12**, 033014.
- [100] Falkovsky, L. A., and A. A. Varlamov, 2007, "Space-time dispersion of graphene conductivity," *Eur. Phys. J. B* **56**, 281.
- [101] Suhas, K., "Modelling Studies and Fabrication Feasibility with LTCC for Non-Conventional RF MEMS Switches," 2007, IISC.
- [102] Fang, Zheyu, Sukosin Thongrattanasiri, Andrea Schlather, Zheng Liu, Lulu Ma, Yumin Wang, Pulickel M. Ajayan, Peter Nordlander, Naomi J. Halas, and F. Javier García de Abajo, 2013, "Gated Tunability and Hybridization of Localized Plasmons in Nanostructured Graphene," *ACS Nano* **7**, 2388.
- [103] Farjam, M., and H. Rafii-Tabar, 2009, "Comment on "Band structure engineering of graphene by strain: First-principles calculations"," *Phys. Rev. B* **80**, 167401.
- [104] S. Kumar, *et al.*, 2013, "Local temperature redistribution and structural transition during Joule-heating-driven conductance switching in VO<sub>2</sub>," *Advanced Materials*, 25, 6128.
- [105] Faugeras, C., M. Amado, P. Kossacki, M. Orlita, M. Kühne, A. A. L. Nicolet, Yu. I. Latyshev, and M. Potemski, 2011, "Magneto-Raman Scattering of Graphene on Graphite: Electronic and Phonon Excitations," *Phys. Rev. Lett.* **107**, 036807.
- [106] Faugeras, C., M. Amado, P. Kossacki, M. Orlita, M. Sprinkle, C. Berger, W. A. de Heer, and M. Potemski, 2009, "Tuning the Electron-Phonon Coupling in Multilayer Graphene with Magnetic Fields," *Phys. Rev. Lett.* **103**, 186803.
- [107] Suhas, K, Sripadaraja, K, 2008, "Mechanical modeling issues in optimization of dynamic behavior of RF MEMS switches," *Int. J. Comp. Inform. Syst. Sci. Eng.*, 221-225.
- [108] Fei, Z., *et al.*, 2012, "Gate-tuning of graphene plasmons revealed by infrared nano-imaging," *Nature (London)* **487**, 82.
- [109] Fei, Z., *et al.*, 2013, "Electronic and plasmonic phenomena at grain boundaries in chemical vapor deposited graphene," *Nat. Nanotechnol.* **8**, 821.
- [110] Fei, Zhe, Yi Shi, Lin Pu, Feng Gao, Yu Liu, L. Sheng, Baigeng Wang, Rong Zhang, and Youdou Zheng, 2008, "High-energy optical conductivity of graphene determined by reflection contrast spectroscopy," *Phys. Rev. B* **78**, 201402.
- [111] Fei, Zhe, *et al.*, 2011, "Infrared Nanoscopy of Dirac Plasmons at the Graphene-SiO<sub>2</sub> Interface," *Nano Lett.* **11**, 4701.
- [112] Kumar, S., 2012, "Types of atomic/nuclear batteries," Stanford University, <http://large.stanford.edu/courses/2012/ph241/kumar1/>
- [113] Feldman, Benjamin E., Jens Martin, and Amir Yacoby, 2009, "Broken-symmetry states and divergent resistance in suspended bilayer graphene," *Nat. Phys.* **5**, 889.
- [114] Ferrari, A. C., *et al.*, 2006, "Raman Spectrum of Graphene and Graphene Layers," *Phys. Rev. Lett.* **97**, 187401.
- [115] Ferrari, Andrea C., 2007, "Raman spectroscopy of graphene and graphite: Disorder, electron-phonon coupling, doping and nonadiabatic effects," *Solid State Commun.* **143**, 47.
- [116] S. Kumar, *et al.*, 2015, "Characterization of electronic structure of periodically strained graphene," *Applied Physics Letters*, 107, 183507.
- [117] Filleter, T., J. L. McChesney, A. Bostwick, E. Rotenberg, K. V. Emtsev, Th. Seyller, K. Horn, and R. Bennewitz, 2009, *Phys. Rev. Lett.* **102**, 086102.
- [118] Fogler, M. M., F. Guinea, and M. I. Katsnelson, 2008, "Pseudomagnetic Fields and Ballistic Transport in a Suspended Graphene Sheet," *Phys. Rev. Lett.* **101**, 226804.
- [119] Fogler, Michael M., 2004, "Nonlinear screening and percolative transition in a two-dimensional electron liquid," *Phys. Rev. B* **69**, 121409.
- [120] Fogler, Michael M., 2009, "Neutrality Point of Graphene with Coplanar Charged Impurities," *Phys. Rev. Lett.* **103**, 236801.
- [121] Forbeaux, I., J.-M. Themlin, and J.-M. Debever, 1998, "Heteroepitaxial graphite on 6H-SiC(0001): Interface formation through conduction-band electronic structure," *Phys. Rev. B* **58**, 16396.
- [122] Suhas, K, 2010, "Materials and processes in 3D structuration of low temperature cofired ceramics for meso-scale devices," *Industrial Ceramics*, **30(1)**.

- [123] Foster, Matthew S., and Igor L. Aleiner, “Graphene via large N: A renormalization group study, 2008,” *Phys. Rev. B* **77**, 195413.
- [124] Gallagher, Patrick, Kathryn Todd, and David Goldhaber-Gordon, 2010, “Disorder-induced gap behavior in graphene nanoribbons,” *Phys. Rev. B* **81**, 115409.
- [125] Gangadharaiah, S., A. M. Farid, and E. G. Mishchenko, 2008, “Charge Response Function and a Novel Plasmon Mode in Graphene,” *Phys. Rev. Lett.* **100**, 166802.
- [126] Gao, Li, Jeffrey R. Guest, and Nathan P. Guisinger, 2010, “Epitaxial Graphene on Cu(111),” *Nano Lett.* **10**, 3512.
- [127] Gerke, A, Kumar S., Provine, J., Saraswat K., “Characterization of metal-nitride films deposited by the Savannah ALD system,” Stanford University.
- [128] Geim, A. K., 2009, “Graphene: Status and Prospects,” *Science* **324**, 1530.
- [129] Geim, A. K., and I. V. Grigorieva, 2013, “Van der Waals heterostructures,” *Nature (London)* **499**, 419.
- [130] Aslani, M., Garner, C. M., Kumar, S., Nordlund, D., Pianetta, P., Nishi, Y., 2015, “Characterization of electronic structure of periodically strained graphene,” *Appl. Phys. Lett.* **107** (18), 183507.
- [131] Geim, A. K., and K. S. Novoselov, 2007, “The rise of graphene,” *Nat. Mater.* **6**, 183.
- [132] George, Paul A., Jared Strait, Jahan Dawlaty, Shriram Shivaraman, Mvs Chandrashekhar, Farhan Rana, and Michael G. Spencer, 2008, “Ultrafast Optical-Pump Terahertz-Probe Spectroscopy of the Carrier Relaxation and Recombination Dynamics in Epitaxial Graphene,” *Nano Lett.* **8**, 4248.
- [133] Georgiou, T., L. Britnell, P. Blake, R. V. Gorbachev, A. Gholinia, A. K. Geim, C. Casiraghi, and K. S. Novoselov, 2011, “Graphene bubbles with controllable curvature,” *Appl. Phys. Lett.* **99**, 093103.
- [134] Ghosh, S., I. Calizo, D. Teweldebrhan, E. P. Pokatilov, D. L. Nika, A. A. Balandin, W. Bao, F. Miao, and C. N. Lau, 2008, “Extremely high thermal conductivity of graphene: Prospects for thermal management applications in nanoelectronic circuits,” *Appl. Phys. Lett.* **92**, 151911.
- [135] Gibertini, Marco, Andrea Tomadin, Marco Polini, A. Fasolino, and M. I. Katsnelson, 2010, “Electron density distribution and screening in rippled graphene sheets,” *Phys. Rev. B* **81**, 125437.
- [136] Gierz, Isabella, Jürgen Henk, Hartmut Höchst, Christian R. Ast, and Klaus Kern, 2011, “Illuminating the dark corridor in graphene: Polarization dependence of angle-resolved photoemission spectroscopy on graphene,” *Phys. Rev. B* **83**, 121408.
- [137] Kumar, S., 2012, “On the Thermoelectrically Pumped LED,” Stanford University, <http://large.stanford.edu/courses/2012/ph250/kumar2/>
- [138] Gierz, Isabella, Christian Riedl, Ulrich Starke, Christian R. Ast, and Klaus Kern, 2008, “Atomic Hole Doping of Graphene,” *Nano Lett.* **8**, 4603.
- [139] Giovannetti, G., P. A. Khomyakov, G. Brocks, V. M. Karpan, J. van den Brink, and P. J. Kelly, 2008, “Doping Graphene with Metal Contacts,” *Phys. Rev. Lett.* **101**, 026803.
- [140] Giovannetti, Gianluca, Petr A. Khomyakov, Geert Brocks, Paul J. Kelly, and Jeroen van den Brink, 2007, “Substrate-induced band gap in graphene on hexagonal boron nitride: *Ab initio* density functional calculations,” *Phys. Rev. B* **76**, 073103.